Science and Justice 53 (2013) 60–66

Contents lists available at SciVerse ScienceDirect

Science and Justice

journal homepage: www.elsevier.com/locate/scijus

Technical note

Automated shape annotation for illicit tablet preparations: A contour angle based classification from digital images

Martin Lopatka [a,1], Wiger van Houten [b,*,2]

[a] Department of Illicit Drugs, Laan van Ypenburg 6, 2497 GB The Hague, The Netherlands
[b] Department of Digital Technology and Biometrics, Laan van Ypenburg 6, 2497 GB The Hague, The Netherlands

ARTICLE INFO

Article history:
Received 28 July 2011
Received in revised form 30 May 2012
Accepted 1 June 2012

Keywords:
Illicit tablets
Ecstasy (XTC)
Image processing
Shape classification
Contour angle
Decision tree

ABSTRACT

In order to facilitate forensic intelligence efforts in managing large collections of physical feature data pertaining to illicit tablets, we have developed an automated shape classification method. This approach performs categorical shape annotation for the domain of illicit tablets. It is invariant to scale, rotation and translation and operates on digital images of seized tablets. The approach employs two processing levels. The first (coarse) level is being based on comparing the contour curvature space of tablet pairs. The second (fine) level is a rule based approach, implemented as a classification tree, that exploits characteristic similarities of shape categories. Annotation is demonstrated over a collection of 169 tablets selected for their diverse shapes with an accuracy of 97.6% when 19 shape categories are defined.

1. Introduction

Described herein is an image processing application providing automated shape categorization for digital photographs of illicit tablets. This method facilitates the high speed organization of tablet seizures into categories based on the tablet shape. Shape categories are derived from the American Pharmacists' Association Compression Tableting Handbook [1]. By the use of discrete, well defined categories, tablet form information can be reliably integrated into database systems to filter search results by tablet shape, thus significantly reducing the number of viable candidates considered in a retrieval procedure. This is particularly effective when a new seizure is non-circular.

Many tablet indexing services, both commercial (IDPD, Epocrates, Ident-A-Drug), and public (pillreport.com, ecstasydata.org, erowid.org, PharmInfoNet) provide some form of search functionality using user-annotated physical descriptions of tablet properties. These descriptions often include the shape of the tablet but are highly unreliable due to inconsistencies in naming convention.

The use of discrete physical properties for evidential value has been treated with increasing interest [2–4] as the illicit market has shown signs of increased physical diversification in illicit XTC tablets [2,5,6]. These physical features have been shown to have substantial evidential value in linking different seizures to a common production batch [3,7]. In practical situations, the shape feature can be most useful as a tool for forensic intelligence applications, drastically reducing the probable candidate tablets when attempting to establish production-batch level links.

With the development of widespread international collaborations such as the European Drug Profiling System (EDPS) [8,9], combined with an increasing emphasis on forensic data collection, reliable and automated feature extraction is more important than ever. Shape information is one of several physical features being extracted in an automated manner under the umbrella of such projects [2,7,9,5,3]. The combined evidence of these features, especially when the features are known to be independent, drastically improves forensic intelligence.

2. Previous methods

Shape classification, specifically in a template matching context, is a well developed field. Early algorithmic approaches achieved impressive results in the respective paradigms being considered [10–13]. In the case of illicit tablets, contours lack highly distinctive inflection points as seen in Mehtre's trademark logos [10] and Chen's country maps [13]. The tablet images are rather impoverished in terms of sharp contour points. We must rather rely on detection of subtle transitions in curvature.

* Corresponding author at: Department of Digital Evidence, Criminal Investigation Unit North, Schweitzerlaan 1, 9728 NR Groningen, The Netherlands. Tel.: +31 881671512, +31 708886666; fax: +31 881671523, +31 708886555.
E-mail addresses: m.lopatka@nfi.minvenj.nls (M. Lopatka), wawvanhouten@gmail.com (W. van Houten).
[1] Tel.: +31 708886666; fax: +31 708886555.
[2] Previous address:

1355-0306/$ – see front matter
doi:10.1016/j.scijus.2012.06.001

We compare the performance of other shape classification methods on our dataset to arrive at a baseline for performance comparison. The classification errors incurred with different methods provide some insight into the functioning of each approach. At the same time we are able to observe specific cases where distinctive tablet categories lack sufficient information to be clearly distinguished. These methods are briefly described in the following sections. Details on the classification performance of these methods are used as a baseline with which we evaluate our own method.

2.1. Curvature scale space

Curvature scale space (hereafter abbreviated to CSS) [14] works by successively blurring the contour of a (binary) image with a one-dimensional Gaussian kernel of width σ, where the kernel width is increased until no points of inflection remain. The location of these inflection points is the distinctive features. For shapes with a high number of these inflection points, such as marine animals, the performance [15] exceeds that observed when using Fourier descriptors and moment invariants (see next sections). The tablets in the current dataset, however, generally have no points of inflection. That is, the boundaries of these tablets can generally be traced without changing direction. Hence, the CSS approach fails to identify many distinctive features thus limiting its use in tablet shape recognition.

2.2. Fourier descriptors

Alternatively, Fourier descriptors [16] can be used to describe the boundary of a shape. Fourier descriptors can be calculated by first extracting N points from the contour of a (binary) image, giving coordinates (x_k, y_k), with $0<k<N-1$. These two-dimensional coordinates can be changed into one-dimensional coordinates, by forming $z(k) = x(k) + \imath y(k)$. Now, taking the Fourier transform of $z(k)$ gives us the Fourier descriptors of the contour. Because the global contour of the image is now represented as a low frequency signal, we remove the higher frequencies. This makes the descriptor more robust, as high frequency disturbances are removed.

2.3. Image moments

Different types of image moments exist. The raw image moments can, for example, be used to calculate the area of a binary image, as well as its center of mass. Invariant image moments are used to describe certain characteristics of an image, insensitive to specific affine transformations. This is further discussed in Section 3.5.2. Image moments have been used extensively for image analysis, object recognition and pattern recognition [17]. Some well-known applications are: optical character recognition [11,18], plant–leaf recognition [19], vehicle detection in satellite images [20], and detecting and localizing duplicated areas in digital images [21]. We used the methods described in [17] to calculate the moments invariant to translation, rotation and scaling for our dataset.

3. Materials and methods

3.1. Image pre-processing

All illicit tablets referred to in this paper were drawn from the collected police seizures currently warehoused at the Netherlands Forensic Institute (NFI). All illicit tablets were photographed from above, against a black background, under a 5000 K illuminant inside a digital imaging lightbox. The photographs were taken using a Nikon D90 camera and a Nikkor 105 mm macro lens. In order to speed up subsequent processing steps, the images were cropped to eliminate as much of the background as possible. Grayscale conversion was performed by calculating a weighted sum of the three color channels (weighted by firmware specified intensity multipliers). Then Otsu threshold selection [22] was used to determine the optimal threshold for image binarization and applied. Finally an erosion filter [23] was applied to the binary image to remove dust speckles and smooth the edges. Each pixel was grouped into a series of connected regions. The largest of these regions was deemed to be the background and the second largest was assumed to be the tablet. All pixels in the second largest fully-connected region received the label of 1 and all other pixels are labeled 0. Subsequently, unconnected regions in the binary image were removed by setting each pixel to 1 if the majority of the pixels in its 3×3 neighborhood were 1. Otherwise, the pixel was set to 0. This served to include dark patches on the tablet surface that may have been excluded by the previous step. The result of this process is an image mask isolating the tablet surface, as seen in Fig. 1.

3.2. The dataset used

Due to the relative rarity of non-circular tablets found in police seizures, we have opted to evaluate this method against two collections of seizures. The first, henceforth referred to as the *selective* data set, consists of 169 tablets selected from the available archive for their diverse shapes; 165 of which belong to the 19 defined shape categories. These are used to evaluate shape category discrimination for our method as well as the known shape classification methods described in Section 2. Additionally, 4 *complex* tablets are included in the selective data set used to test our own method to determine whether these tablets could, in principal be identified as abnormal. Again, due to the rarity of non-circular tablets, the amount of tablets for the diverse shapes listed in Table 2 is limited. A class balanced data set is impossible since we use only genuine illicit tablets seized in the Netherlands.

The second data set, the *non-selective* data set, consists of a random selection of tablets drawn directly from one year of police seizures in the Netherlands. Both small-scale and large-scale seizures are included, and the total number of tablets in this case is 774. This represents an unbiased dataset that is representative for a typical years' worth of seizures. Every tablet in both data sets has been manually annotated by a single forensic researcher in accordance with the APA standards so that a ground truth is available.

3.3. Tablet shape templates

In order to classify these tablets we must define ideal tablet shapes. For this we use binary templates derived from images of tableting punches, published in the American Pharmacists' Association guide [1]. These can be seen in Fig. 2. These shape categories are well formed, in that concise differentiation between any two groups can be expressed in terms of rule-like descriptions. For example, the *arc-triangle* shape may not contain any edge such that the tangent to this edge has an angle of zero, differentiating it from the *triangle* shape.

3.4. Contour angle vector representation (CAV)

After successfully processing the tablet images, by the method described in Section 3.1, so as to leave only a binary representation of the tablet surface, the contours of this binary image were traced to obtain a closed boundary of equidistant points. This process was performed using a radial sweep algorithm [24] such that each point along the boundary is connected (8-neighbor) with the next point in the contour. The tablet boundary was then extracted in sequential order starting at the upper left corner of the binary image. The contour is resampled to a fixed number of equally spaced points N. This process was performed so that the points are linearly equidistant in terms of their index along the contour. This value for N should be large enough

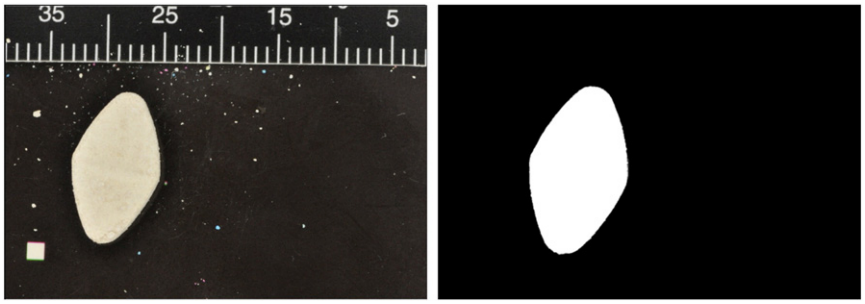

Fig. 1. By thresholding the original image (left) and removing unconnected regions, a binary representation of the tablet is obtained (right).

to avoid influence of the exact placement of these points, and small enough to be fast. In our experiments we used $N = 1000$.

This contour may show irregularities due to damage to the tablet. To prevent these irregularities from showing up in the contour angle representation, a convolution with a Gaussian kernel of width W and standard deviation σ are applied to the contour. We used $W = 15$ and $\sigma = 1.5$. This approach is inspired by earlier work in curvature scale space [25,26].

For each point (x_i, y_i) in the contour extracted from the image, the subtended angle is calculated between the vectors $\mathbf{v}_1 \equiv (x_i, y_i) - (x_{i-m}, y_{i-m})$ and $\mathbf{v}_2 \equiv (x_i, y_i) - (x_{i+m}, y_{i+m})$. Here, m denotes a certain distance *along the contour* from (x_i, y_i). The best performance may be achieved by selecting a value for m dependent on the original resolution of the image and the N value, such that characteristic inflection points in the contour are preserved while rough edges in the material are smoothed. Since small image details (e.g. surface disaggregation) are not informative in a closed class categorization of this type, we use a value of 1000 points for N with an m value of 100.

The angle was calculated from the cosine trigonometric rule, shown in its vector form by Eq. (1).

$$\alpha = cos^{-1}\left(\frac{\mathbf{v}_1 \cdot \mathbf{v}_2}{\|\mathbf{v}_1\|\|\mathbf{v}_2\|}\right) \tag{1}$$

Instead of using the angle values directly, we used the complement of this angle: $\alpha' = 180 - \alpha$. Hence, continuous straight edges will have a contour angle of 0°.

By calculating this angle for each point along the contour, we were able to represent the image as a one dimensional vector of angles. An example of the contour angle of the *heart* shape is shown in Fig. 3, where we have used $N = 1000$ equidistant points along the contour, and $m = 100$. Because we use a fixed number of equidistant points for representing the contour, the contour angle is scale invariant. Due to the fact that the radial sweep algorithm [24] derives contour points starting at the lower left corner of the image frame our transform from the binary tablet image to the CAV representation is also invariant to translation within the frame. If a tablet image is rotated, the contour angle may simply be shifted in the contour-angle space.

3.5. Shape label assignment

The label assignment occurs in two separate stages. Based on the mean square error between a set of templates and an unknown tablet, the basic shape is estimated. As some shapes are highly similar, a second examination determines the exact shape. In the following sections each step is explained in detail.

3.5.1. Coarse (first) level shape classification

The contour angle was calculated for all 19 template shapes and the candidate tablet. Candidate label assignment was performed based on finding which CAV representation of the templates minimizes the mean square error with the CAV representation of the candidate tablet. The label assigned to the candidate tablet equals the label of the template which produces the lowest mean square error. This will be referred to as the candidate label. The contour angle is scale invariant due to the fixed number of points N, but not rotation invariant. Because the orientation of the candidate tablets is unknown at the time of photography, we must calculate the mean square error for each possible rotation of the candidate tablet relative to the fixed orientation template. This was accomplished by circularly shifting the contour angle representation from $1 \ldots N$. After each shift the MSE is calculated again, the lowest of the $1 \ldots N$ error values is considered as the true error between a candidate tablet and the template. In this way invariance to rotation was achieved. For any tablet where

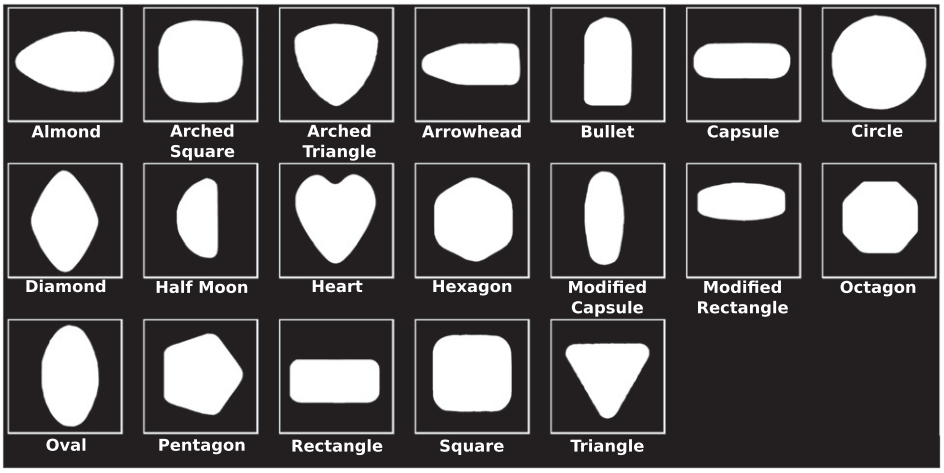

Fig. 2. The 19 ideal tablet shape templates from the American Pharmacists' Association guide [1].

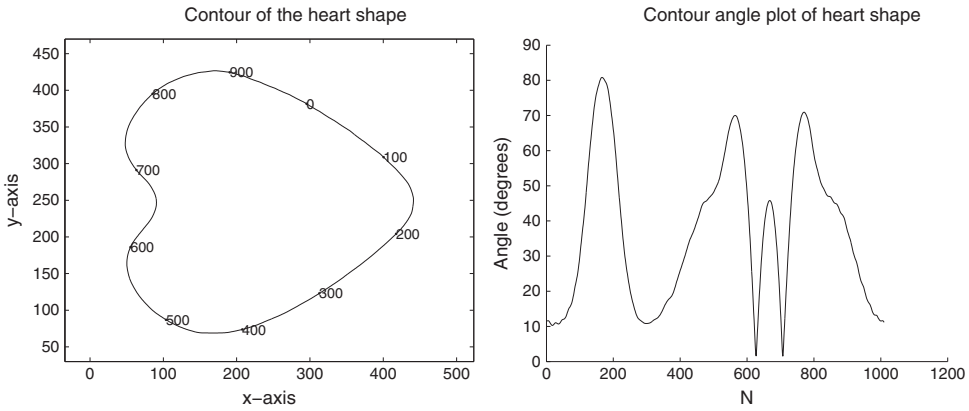

Fig. 3. Extracted contour from a heart-shaped tablet (left), and its contour angle representation (right). Labeled points along the contour in the left figure correspond to the numbers on the x-axis in the right figure.

the lowest MSE score was greater than 200 the *complex* label is automatically assigned. This label is reserved for non-standard custom made tablet punches which can take any form.

Certain classes were found to be highly prone to error when only the CAV representation is considered. In many cases the shape category may be contingent only on the curvature (or lack thereof) of the short side of the tablet. However, by definition, these shapes have distinct characteristics. When a confident classification was unreliable exclusively by matching to the lowest MSE, further information was derived from patterns within the similarity or difference to multiple templates. For example, a tablet quite similar to the template of *arc triangle*, that still fails to reach a sufficiently low MSE score may be more confidently classified if it also has a low MSE score against the *heart* and *triangle* templates.

Fig. 4 depicts the overall execution of this classification.

3.5.2. Fine (second) level shape classification

Some of the distinguishing properties between shapes may fall below the discriminative ability of a CAV driven model using only a *best-match* criterion. For this a rule-based, second pass classification was employed. Similar second level refinements in closed set shape classification have shown a promise in the use of geometric properties [27]. Rather than encode a rule based classification scheme exclusively for exceptional cases, we used the MSE scores that each tablet was assigned when compared with each template as the feature vector to train a classification tree. The modeling was performed using the Matlab ™classregtree package and methods described in [28] were followed.

The tablets initially easily classified based solely on the *best-match* criterion (described in Section 3.5.1) were still classified based on minimal MSE scorings. These rules are naturally encoded in the classification tree as early terminal nodes. More difficult classifications

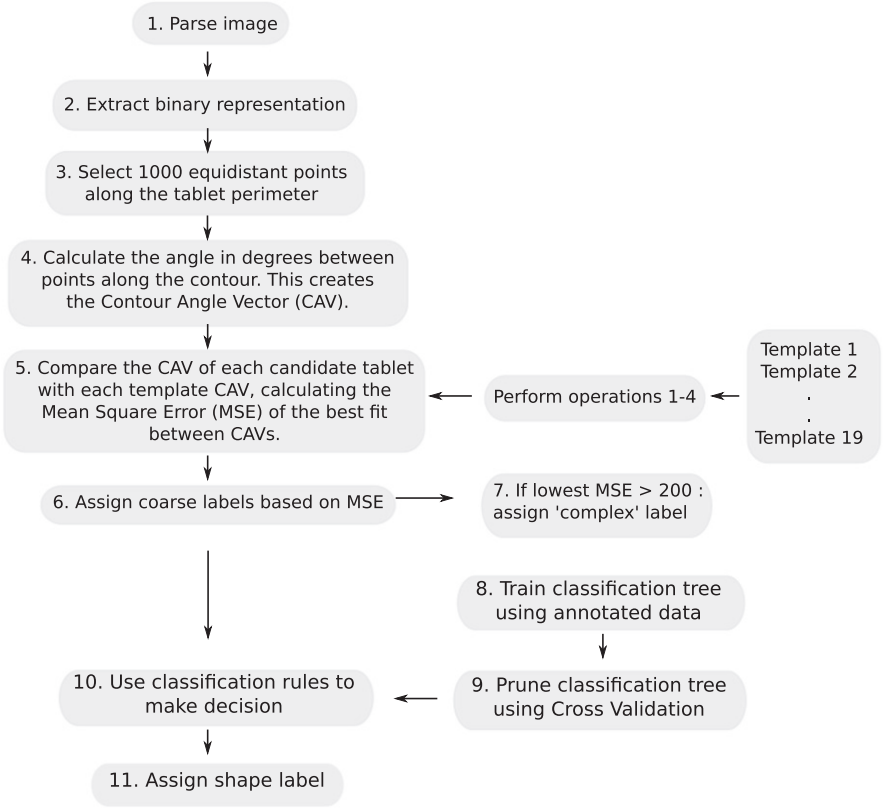

Fig. 4. Execution of the classification method.

were defined by later occurring terminal nodes in the tree that take into account multiple MSE scores to classify candidate tablets by their (dis)similarity to multiple templates. For example, a tree trained on a subset of the combined data sets (*non-selective* and *selective*) demonstrated a late terminal node for assignment of the *heart* label that requires a candidate tablet meet the conditions shown in Table 1.

In this way *hard* cases were considered using more information regarding their (dis)similarity with multiple template shapes. In the example shown in Table 1 the variables x*n*, correspond to MSE scores against different template shapes. It is clear that the definition of a shape category employs similarity to specific templates as well as required difference to others. The classification tree used in the fine level classification was trained on a subset of data containing at least one example of each class. Pruning conditions were defined such that each class is represented by at least one terminal node [29]. The tree in Fig. 5 is an example of a fully trained classification tree that takes into account multiple MSE scores to specific shape tablets in order to classify hard cases correctly. The specific tree structure will always depend on the data used for training. However, multiple morphologies can achieve equal classification performance. Note that a classification tree may have multiple terminal nodes with the same label.

The experiments used to evaluate the classification performance of this approach used the *selective* data set described in Section 3.2. All branching thresholds used in the classification tree were derived from a training run using a subset of data including at least one example of each shape. The splitting criterion selected was the Gini diversity index [30,28] and pruning was restricted to ensure that a minimum of one terminal node per class was preserved. Optimization of the tree size was based on minimum classification error in a hold-one-out validation method.

4. Results

In each case the resulting performance was achieved in a hold-one-out paradigm, where all available data belonging to selected data set were used for training the tree, save the point being evaluated.

The *selective* collection of 169 tablets was processed by precisely the workflow depicted in Fig. 4. The overall performance over this collection, when each tablet is considered equally likely, was a correct classification of 165 of 169 (97.6%) tablets correctly annotated. The results are presented in Table 2. We also evaluated the methods briefly discussed in Section 2. These methods for shape classification have been implemented as described in the cited references. The same preprocessing steps were used to ensure fair comparison. The performance for a Fourier Descriptor method, Image Moment method and Contour Angle Vector method without fine level refinement are shown in Table 2.

In the case of the Fourier descriptors, classification was based on the minimum Euclidean distance between the Fourier descriptor of a candidate tablet F_c and the Fourier descriptor of each of the 19 template tablets F_{t_i}. We exclude the *complex* shape tablets from this experiment. We note that the FD method has difficulty in distinguishing roughly similar shapes from one another. In particular, all capsules were wrongly classified as either *rectangle* or *modified capsules*. Likewise, wrongly classified *diamonds* were seen as *ovals*, and *heart* shapes were frequently seen as either *triangles* or *arc triangles*.

Table 1
Example conditions at late terminal node.

152.615<x1<730.813
52.8811<x2
55.7816<x3
662.297<x4<1389.28
610.037<x5
33.1131<x7
153.351<x8
227.414<x10
735.127<x16
160.234<x17
327.307<x19

Classification using the invariant image moments was also performed by a template matching procedure where the metric used is again minimum Euclidean distance. The performance observed from the image moments was worse than that of the Fourier descriptors. In particular, all almonds were classified as diamonds. *Capsules* were classified as either *arrowhead*, *half-moon* or *modified rectangle*. Other examples include squares classified as *arc triangles*, and *hearts* frequently misclassified as either *arc triangle*, *square* or *triangle*.

The CAV approach (without fine level refinement) performs comparatively well. The misclassified heart tablets were all classified as *arc triangle*, and the misclassified *modcapsules* were classified as *modrectangle*. Finally, rectangles were frequently detected as capsules. All these errors are predictable as these shapes are very similar. This prompted us to use the fine level refinement, as explained in 3.5.2. The results for the CAV approach including the fine level refinements are listed in the final column of Table 2.

The refined CAV method performance was 97.6% correct annotation. We scale these results by the relative class frequencies so that errors within a class are weighted equally. This yields a class normalized performance of 95% to account for the imbalances observed in the available tablet classes. The errors observed were in the *complex*, *oval*, and *heart* classes. In the *complex* case, the tablets were incorrectly classified as *heart* tablets. The remaining two errors observed were an *oval-diamond* misclassification and a *heart-complex* misclassification. An example of an incorrectly classified tablet is shown in Fig. 6.

We then evaluated the applicability of the fully trained classification tree to a previously blind data set. This was to assess whether overfitting has occurred in the classification tree. The tablets in the *non-selective* data collection have *not* been involved in the system tuning and as a random selection of case samples, the class frequencies were expected to represent the actual occurrence of specific shapes in the illicit market. Our method was applied to this collection of 774 tablets. No errors were observed. The breakdown of classification results is shown in Table 3.

The computation time needed to perform the shape classification with the proposed method can be summarized with the following numbers. Generating the CAV representation of a binary image takes approximately 0.2 s on an Intel 2.0 GHz Core2Duo PC, whereas classification of a tablet takes an average additional 0.3. All methods were implemented in Matlab v7.8.0 (2009a).

5. Discussion

As with any categorization problem, there are often gray areas. By using templates which define the archetypal exemplar of a specific shape, we can formulate the problem of classification in terms of measuring the similarity to each template. This is precisely what is being done in the coarse level classification described in Section 3.5.1. However, in such cases, the results achieved often depend on what aspects of the samples and templates one chooses to observe as well as which measure of similarity one uses. It is easy to understand how the freedom to select both the measurements and the categories themselves can lead to artificially high performance. For this reason we used a recognized standard for the shape categories. In order to avoid overfitting, which rule-based systems are highly prone to [31], we maintain a hold-out validation set with which to determine the true performance.

Ultimately the usefulness of this approach will be defined by the forensic context in which it is used. If a candidate tablet is circular, then the advantages of limiting a query by shape are negligible. However, due to the relatively infrequent distribution of non-circular tablets in the environment, an accurately annotated tablet shape can prove very useful in limiting the list of potential candidate matches.

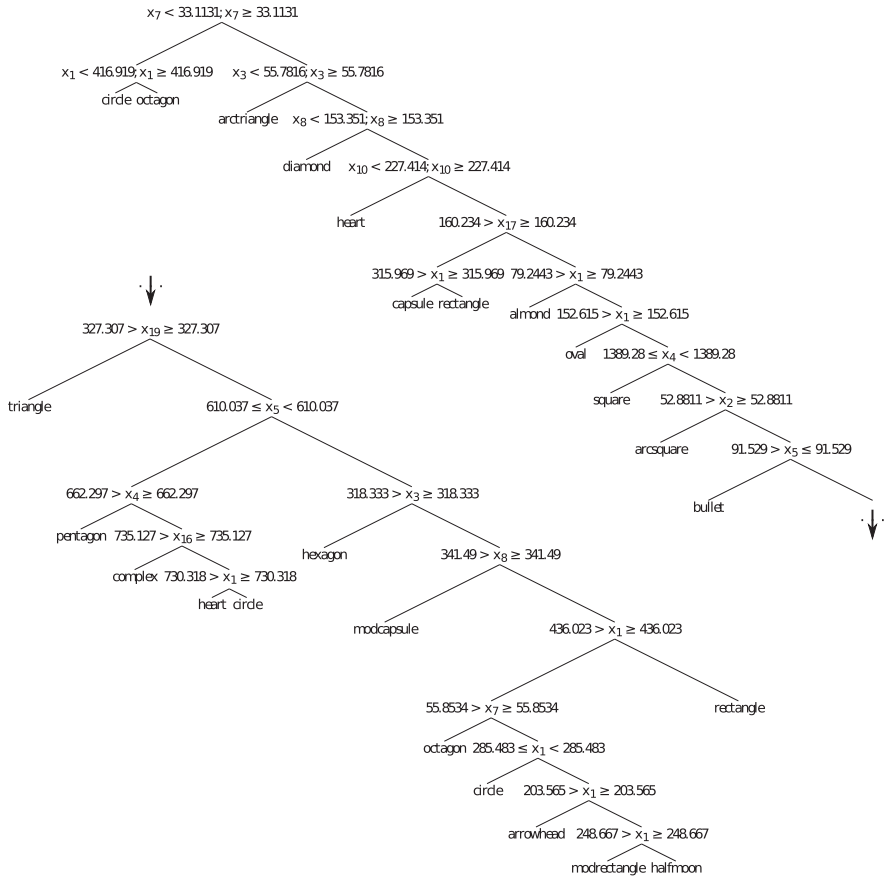

Fig. 5. Classification tree trained on a subset of combined data sets.

The cost of a non-circular tablet being incorrectly assigned the label of *circle* is very high, since this would lead to the tablet being considered among the most common tablet shape. In a data base, the potential advantages of being able to limit a search by *shape* when the candidate seizure is non-circular, are drastic in terms of computation as well as practical matters.

Table 2
Classification performance of the Fourier Descriptor method (FD), Contour Angle Vector without fine level refinement (CAV) and Image Moment (IM) method, over selectively diverse tablet collection. The 'Refined CAV' column lists the classification performance with the fine level refinements. Numbers in square brackets are the number of correct classifications. For the FD and IM methods, no routines were included for detecting complex shapes (denoted in the table with †).

Shape	FD	CAV	IM	Refined CAV
Almond	[3/4] 75%	[4/4] 100%	[0/4] 0%	[4/4] 100%
Arc square	[3/3] 100%	[3/3] 100%	[3/3] 100%	[3/3] 100%
Arc triangle	[36/37] 97%	[37/37] 100%	[37/37] 100%	[37/37] 100%
Arrowhead	[2/2] 100%	[2/2] 100%	[2/2] 100%	[2/2] 100%
Bullet	[4/4] 100%	[4/4] 100%	[4/4] 100%	[4/4] 100%
Capsule	[0/10] 0%	[10/10] 100%	[0/10] 0%	[10/10] 100%
Circle	[31/32] 97%	[32/32] 100%	[31/32] 97%	[32/32] 100%
Diamond	[16/25] 64%	[25/25] 100%	[16/25] 64%	[25/25] 100%
Half moon	[2/2] 100%	[2/2] 100%	[0/2] 0%	[2/2] 100%
Heart	[11/21] 52%	[14/21] 67%	[11/21] 52%	[11/12] 75%
Hexagon	[2/2] 100%	[2/2] 100%	[0/2] 0%	[2/2] 100%
Mod capsule	[1/2] 50%	[0/2] 0%	[0/2] 0%	[2/2] 100%
Mod rectangle	[2/2] 100%	[2/2] 100%	[0/2] 0%	[2/2] 100%
Octagon	[3/3] 100%	[3/3] 100%	[0/3] 0%	[3/3] 100%
Oval	[2/4] 50%	[2/4] 50%	[0/4] 0%	[3/4] 75%
Pentagon	[2/2] 100%	[2/2] 100%	[2/2] 100%	[2/2] 100%
Rectangle	[1/3] 33%	[1/3] 33%	[1/3] 33%	[3/3] 100%
Square	[4/4] 100%	[4/4] 100%	[0/4] 0%	[4/4] 100%
Triangle	[3/3] 100%	[3/3] 100%	[3/3] 100%	[3/3] 100%
Complex	†	[2/4] 50%	†	[2/4] 50%
Overall	[128/165] 78%	[154/169] 91%	[110/165] 67%	[165/169] 98%

We have mentioned that due to the rarity of non-circular tablets in the illicit market, we are faced with an unbalanced data set. At this time the acquisition of more data is impossible. We have considered the use of pharmaceutical tablets, but it is the opinion of many forensic experts that professionally manufactured pharmaceutical tablets are not comparable with illicit tablets in terms of quality and contour smoothness. We hope to evaluate the performance over the more rare shaped tablets as further police seizures are made.

Independent of considerations about the appropriateness of specific categories and the justifiability of design objectives, the consistency of the system is by far the most important measure. In a well calibrated system, when errors are made and misclassifications occur, it is usually

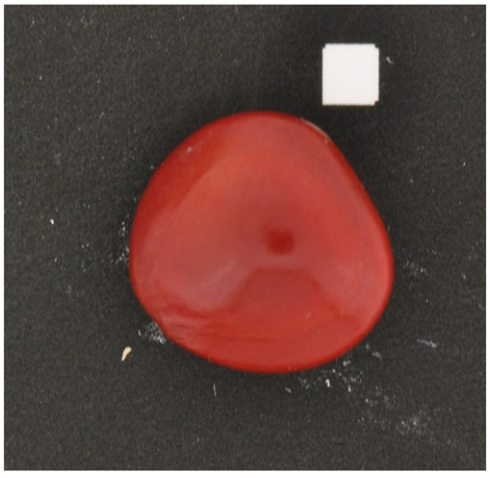

Fig. 6. Tablet belonging to complex class incorrectly classified as heart.

Table 3
Annotation performance for unbiased data set.

Circle	[693/693] 100%
Heart	[10/10] 100%
Square	[2/2] 100%
Capsule	[4/4] 100%
Mod rectangle[a]	[1/1] 100%
Triangle	[2/2] 100%
Arc triangle	[42/42] 100%
Diamond	[20/20] 100%

[a] Unique case tablet used in training and testing.

due to fringe conditions being encountered. As long as these errors are systematic, then the use of shape categories in a database retrieval application serves its purpose, which is to retrieve tablets of a similar shape.

The selection of a classification tree, as well as the methodology employed in its evaluation are motivated by the eventual practical deployment of this application in a practical forensic databasing context. The classification tree can be trained based on virtually any number of tablet seizures and the classification of a new tablet can be performed very quickly since the only information encoded are the rules derived from an annotated training set. The classification of a new tablet will always mimic a leave-one-out paradigm since new tablets are compared individually against the sum total of gathered samples. For these reasons, the method described herein is ideal for the task at hand and the usual risks of overfitting are somewhat negated by the large and representative corpus of training data available.

6. Conclusion

We have developed a system for automated, reliable, high-speed, shape category annotation from overhead digital images of illicit XTC tablets. By using digital image processing techniques described above and borrowing a naming convention from pharmaceutical practices, we are able to use a two step methodology to accurately annotate tablet shape names. The performance over the *selective* collection demonstrates reliability in performance across the full range of shape categories, while the 100% classification accuracy achieved over a representative sample of 1 year of case work speaks for itself. This method can drastically improve forensic XTC tablet cataloging practices in digital databases. The method described is easy, fast, and non-destructive; requiring nothing more than a digital image of a tablet. For this reason, a harmonized method can be easily developed to combine intelligence from multiple forensic and police institutes. This may significantly aid in the global monitoring of the illicit tablet market.

Acknowledgments

We would like to thank the Netherlands Forensic Institute for providing access to their vast collection of illicit tablet seizures. Certainly few collections of this size and quality exist.

References

[1] A. P. Association, Practical Tableting Handbook, 7th rev ed., 2006 (edition).
[2] A. Bolck, C. Weyermann, L. Dujourdy, P. Esseiva, J. van den Berg, Different likelihood ratio approaches to evaluate the strength of evidence of mdma tablet comparisons, Forensic Science International (2009) 42–51.
[3] R. Marquis, C. Delaporte, P. Esseiva, C. Weyermann, L. Aalberg, F. Besacier, J.B. Jr, R. Dahlenburg, C. Kopper, F. Zrcek, Drug intelligence based on MDMA tablets data 2. Physical characteristics profiling, Forensic Science International 178 (2008) 34–39.
[4] C. Aitken, F. Taroni, Statistics and the Evaluation of Evidence for Forensic Scientists, John Wiley & Sons, 2004.
[5] C. Zhing, The Analysis of Ecstasy Tablets in a Forensic Drug Intelligence Perspective, Ph.D. thesis, University of Lausanne, 2005.
[6] Q. Milliet, C. Weyermann, P. Esseiva, The profiling of MDMA tablets: a study of the combination of physical characteristics and organic impurities as sources of information, Forensic Science International (2009) 58–65.
[7] M. Lopatka, M. Vallat, Surface granularity as a discriminating feature of illicit tablets, Forensic Science International 210 (2011) 188–194.
[8] EMCDDA, Annual Report on the State of the Drugs Problem in Europe, European Monitoring Centre for Drugs and Drug Addiction, Lisbon, 2010.
[9] E. Commission, Report from the Commission 2010: Progress Review of the Eu Drugs Action Plan (2009–2012), 2010.
[10] B.M. Mehtre, M.S. Kankanhalli, W.F. Lee, Shape measures for content based image retrieval: a comparison, Information Processing and Management 33 (1997) 319–337.
[11] M.-K. Hu, Visual pattern recognition by moment invariants, IRE Transactions on Information Theory (1962) 179–187.
[12] E. Bribiesca, A. Guzman, How to describe pure form and how to measure differences in shapes using shape numbers, Pattern Recognition 12 (1979) 101–112.
[13] C.-C. Chen, Improved moment invariants for shape discrimination, Pattern Recognition 26 (1993) 683–686.
[14] F. Mokhtarian, A.K. Mackworth, A theory of multiscale, curvature-based shape representation for planar curves, IEEE Transactions on Pattern Analysis and Machine Intelligence 14 (1992) 789–805.
[15] S. Abbasi, F. Mokhtarian, J. Kittler, Curvature scale space image in shape similarity retrieval, Multimedia Systems 7 (1999) 467–476.
[16] E. Persoon, K. Fu, Shape discrimination using fourier descriptors, IEEE Transactions on Systems, Man, and Cybernetics 7 (1977) 170–179.
[17] J. Flusser, T. Suk, B. Zitová, Moments and Moment Invariants in Pattern Recognition, 1st edition John Wiley & Sons, Ltd., 2009
[18] J. Flusser, T. Suk, Affine moment invariants: a new tool for character recognition, Pattern Recognition Letters 15 (1994) 433–436.
[19] X.-F. Wang, D.-S. Huang, J.-X. Dua, H. Xu, L. Heutte, Classification of plant leaf images with complicated background, Applied Mathematics and Computation 205 (2008) 916–926.
[20] L. Eikvil, L. Aurdal, H. Koren, Classification-based vehicle detection in high-resolution satellite images, Journal of Photogrammetry and Remote Sensing 64 (2009) 65–72.
[21] B. Mahdian, S. Saic, Detection of copy-move forgery using a method based on blur moment invariants, Forensic Science International 171 (2007) 180–190.
[22] N. Otsu, A threshold selection method from gray-level histograms, IEEE Transactions on Systems, Man, and Cybernetics 9 (1979) 62–66.
[23] R.M. Haralick, L.G. Shapiro, Computer and Robot Vision, 1 edition Addison-Wesley, 1992.
[24] T. Pavlidis, Algorithms for Graphics and Image Processing, 1st edition Computer Science Press, 1981.
[25] L.J. Latecki, R. Lakamper, Convexity rule for shape decomposition based on discrete contour evolution, Computer Vision and Image Understanding 73 (1999) 441–454.
[26] F. Mokhtarian, Sillouette-based isolated object recognition through curvature scale space, IEEE Transactions on Pattern Analysis and Machine Intelligence 17 (1995) 539–544.
[27] K. Singh, I. Gupta, S. Gupta, Comparison of pnn-pca with svm-bdt and moment based techniques for leaf shape recognition and classification, In: IPCV, 2010, pp. 726–732.
[28] L. Breiman, J. Friedman, C.J. Stone, R.A. Olshen, Classification and Regression Trees, 1st ed. CRC Press, Boca Raton, FL, 1984 (edition).
[29] S.J. Russell, P. Norvig, Artificial Intelligence: A Modern Approach, Pearson Education, 2003.
[30] L. Jost, Entropy and Diversity, Oikos, 2006.
[31] C.M. Bishop, Pattern Recognition and Machine Learning, 2nd edition Springer, 2007.